Operational Influence Proxies in a TFIM Surrogate: Non-Monotonicity and a Controlled $\omega = 0$ Witness Floor Mechanism

Lluis Eriksson
Independent Researcher
lluiseriksson@gmail.com

January 2026

Abstract

We study spatial influence detection in a transverse-field Ising chain (TFIM) subjected to localized Markovian noise. Using an operational one-site trace-distance influence proxy computed from TEBD combined with Monte Carlo wavefunction (MCWF) sampling, we test whether remote dissipation produces an identifiable nonzero asymptotic influence offset (a "floor") as a function of separation ϵ. Uncertainties are estimated by trajectory bootstrap and model selection is performed between exponential decay and exponential-plus-offset forms using both BIC and the finite-sample corrected criterion AICc. In the TFIM surrogate regimes explored, we find no robustly identifiable floor for both dephasing and amplitude-damping channels; instead, the influence proxy is non-monotone in separation, consistent with coherent finite-size structure superimposed on average attenuation. To demonstrate that floors can exist as a controlled mechanism independent of fragile spatial fits, we present a Davies/witness stress test: for nonzero zero-frequency bath weight $\gamma(0) > 0$, a commutator witness yields a strictly positive lower bound on an effective decay envelope. Exact-diagonalization calculations show this lower bound is robust to enlarging the observable support and to variations in inverse temperature.

Contents

1 Introduction

Locality constraints in quantum lattice systems limit how quickly and how strongly perturbations influence distant degrees of freedom [1]. Operational influence detection often relies on reduced-state or local-observable proxies rather than direct access to a full many-body channel. A recurring question is whether such proxies exhibit a nonzero asymptotic offset (a "floor") in separation ϵ, or whether they decay without a detectable offset.

This paper has two goals. First, we evaluate a TFIM numerical surrogate using a one-site trace-distance influence proxy under localized Markovian noise, and we test for an identifiable floor using statistically controlled model selection. Second, we provide a controlled stress test in which a floor mechanism exists in a precise sense: as a witness-based lower bound in a Davies-type $\omega = 0$ sector with $\gamma(0) > 0$ [2, 3, 4]. The contrast clarifies a key message: the existence and detectability of floors depends on both the chosen operational proxy and on low-frequency bath structure.

2 TFIM surrogate: model, proxy, and inference pipeline

2.1 Hamiltonian

We consider a TFIM chain of length N with open boundary conditions and Hamiltonian

$$H \;=\; -J\sum_{i=1}^{N-1} X_i X_{i+1} \;-\; h\sum_{i=1}^{N} Z_i.$$

(This is equivalent to the more common ZZ–X convention by a global basis rotation.)

2.2 Noise channels and geometry

We study localized Markovian noise applied on a set of sites separated from a probe site S by a distance ϵ. We consider two channels:

- Dephasing on selected sites, with jump operators proportional to Z.
- Amplitude damping on selected sites, with jump operators proportional to $\sigma^- = (X - iY)/2$.

For each separation ϵ, noise acts on a small region $\mathcal{N}(\epsilon)$ at distance ϵ from S.

2.3 Operational influence proxy

For each ϵ, we compare (i) a noisy evolution with dissipation applied at $\mathcal{N}(\epsilon)$ to (ii) a clean unitary evolution under H. Let $\bar{\rho}_S^{\text{noisy}}(t)$ be the trajectory-averaged reduced state at the probe site, and $\rho_S^{\text{uni}}(t)$ the reduced state under unitary evolution. We define the instantaneous trace-distance influence

$$D_{\text{tr}}(t;\epsilon) \;:=\; \frac{1}{2}\left\|\bar{\rho}_S^{\text{noisy}}(t) - \rho_S^{\text{uni}}(t)\right\|_1,$$

where $\rho_S^{\mathrm{uni}}(t)$ is computed from the same Hamiltonian evolution for all ϵ (the unitary reference does not depend on ϵ), and the windowed influence proxy

$$D_{\mathrm{tr}}(t;\epsilon) \;:=\; \frac{1}{2}\left\|\bar{\rho}_S^{\mathrm{noisy}}(t) - \rho_S^{\mathrm{uni}}(t)\right\|_1, \qquad \mathcal{A} \in \{\max, \mathrm{mean}, \mathrm{rms}\}.$$

Time windows are chosen in a post–light-cone (LC) manner:

$$t_0(\epsilon) = \alpha\,\epsilon/v, \qquad t_1(\epsilon) = t_0(\epsilon) + \tau.$$

We choose (α, v, τ) so that the analysis window lies beyond the expected arrival time scale ϵ/v for the largest separations considered.

2.4 Uncertainty estimation and model selection

Uncertainties of $D_{\mathrm{tr}}^{\mathcal{A}}(\epsilon)$ are estimated by bootstrap over trajectories (16–84% intervals). We compare two parametric forms:

$$M_{\mathrm{exp}}:\; D(\epsilon) = Ae^{-a\epsilon}, \qquad M_{\mathrm{floor}}:\; D(\epsilon) = D_0 + Ae^{-a\epsilon},$$

with constraints $A \geq 0$ and $D_0 \geq 0$, using weighted least squares with bootstrap-derived pointwise uncertainties and a log-spaced grid search over a. Model preference is summarized by

$$\Delta\mathrm{BIC} = \mathrm{BIC}(M_{\mathrm{floor}}) - \mathrm{BIC}(M_{\mathrm{exp}}), \qquad \Delta\mathrm{AICc} = \mathrm{AICc}(M_{\mathrm{floor}}) - \mathrm{AICc}(M_{\mathrm{exp}}),$$

with

$$\mathrm{BIC} = \chi^2 + k\log n, \qquad \mathrm{AICc} = \chi^2 + 2k + \frac{2k(k+1)}{n-k-1},$$

where n is the number of spatial points and k the number of model parameters [5, 6]. For the tail-only fits reported below ($n = 5$), the AICc finite-sample correction contributes approximately 18 additional units to the offset model relative to the no-offset model ($k = 3$ vs. $k = 2$), so $\Delta\mathrm{AICc} \approx 20$ should be interpreted primarily as insufficient support to justify an extra parameter at small n, rather than as strong physical evidence against D_0.

3 TFIM surrogate results

3.1 Dephasing deep tail ($N = 80$, post–LC)

We analyze the post–LC deep tail for dephasing at $N = 80$ and $\epsilon \in \{16, 20, 24, 28, 32\}$. The measured $D_{\mathrm{tr}}^{\mathcal{A}}(\epsilon)$ is non-monotone in ϵ (a bump appears), indicating coherent finite-size structure superimposed on any average attenuation. Model selection yields "no floor supported/identifiable" for all aggregators:

$D_{\max}:\ \Delta\mathrm{BIC} \approx 1.6,\ \Delta\mathrm{AICc} \approx 20, \qquad D_{\mathrm{mean}}:\ \Delta\mathrm{BIC} \approx 1.5,\ \Delta\mathrm{AICc} \approx 20, \qquad D_{\mathrm{rms}}:\ \Delta\mathrm{BIC} \approx 1.5,\ \Delta\mathrm{AICc} \approx 20$

3.2 Amplitude damping corroboration ($N = 24$)

As a corroborating check in a smaller system and distinct regime, we analyze amplitude damping at $N = 24$ with $\epsilon \in \{2, 4, 6, 8, 10\}$. The dependence of $D_{\mathrm{tr}}^{\mathcal{A}}(\epsilon)$ on ϵ is non-monotone. Model selection favors the no-floor model across aggregators:

$D_{\max}:\ \Delta\mathrm{BIC} \approx 1.6,\ \Delta\mathrm{AICc} \approx 20, \qquad D_{\mathrm{mean}}:\ \Delta\mathrm{BIC} \approx 1.6,\ \Delta\mathrm{AICc} \approx 20, \qquad D_{\mathrm{rms}}:\ \Delta\mathrm{BIC} \approx 1.6,\ \Delta\mathrm{AICc} \approx 20$

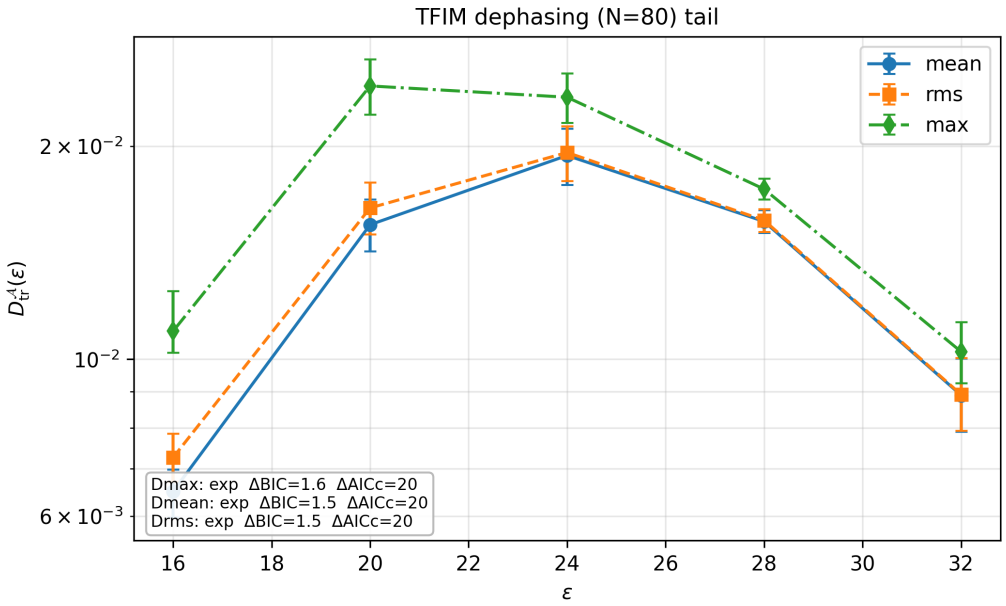

Figure 1: TFIM dephasing tail ($N = 80$): windowed influence proxy $D_{\mathrm{tr}}^{\mathcal{A}}(\epsilon)$ with bootstrap 16–84% intervals. Model selection supports the no-floor model for $\mathcal{A} \in \{\max, \mathrm{mean}, \mathrm{rms}\}$.

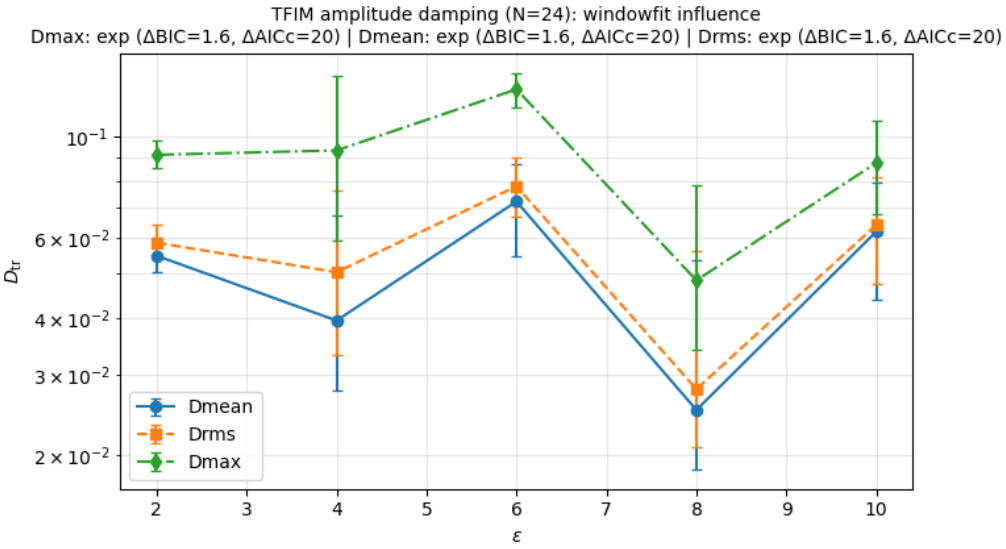

Figure 2: TFIM influence proxy $D_{\mathrm{tr}}^{\mathcal{A}}(\epsilon)$ under amplitude damping ($N = 24$, window-fit protocol). Error bars denote bootstrap 16–84% intervals over trajectories. The dependence on ϵ is non-monotone, consistent with coherent finite-size structure.

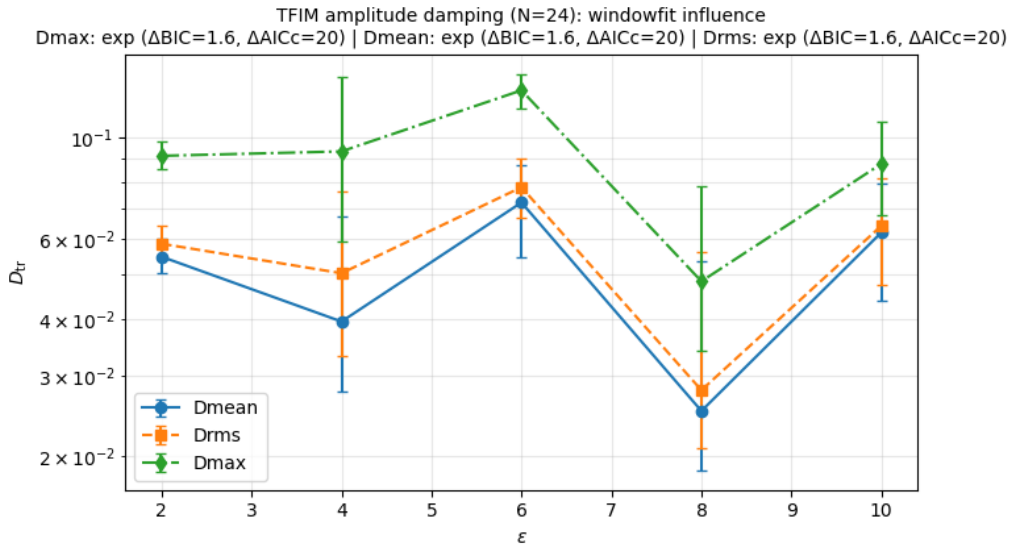

Figure 3: (Optional visualization) Processed influence summary for the amplitude-damping check ($N = 24$).

4 Davies/witness stress test: controlled $\omega = 0$ floor mechanism

4.1 Scope (stress test, not full Davies reconstruction)

Here we use a controlled $\omega = 0$-channel witness (Dirichlet-form identity) as a stress test; we do not attempt to reconstruct the full Davies generator numerically in this section. This section is therefore a certified lower-bound mechanism statement, not a claim about the full ϵ-dependence of physical decoherence rates in the TFIM surrogate.

4.2 Definitions: $S(0)$ and $\mathcal{A}_\epsilon$

Let H be the system Hamiltonian and S the microscopic system–bath coupling operator. We define the $\omega = 0$ component

$$S(0) \;:=\; \sum_n \Pi_n S \Pi_n,$$

where $\{\Pi_n\}$ are spectral projectors of H (energy-block-diagonal part). Although the microscopic coupling S may be local in the site basis, $S(0)$ is defined in the energy basis and is generally nonlocal in real space. We take $\mathcal{A}_\epsilon$ as the span of traceless Pauli strings supported on a block of length L starting at site $k = j_0 + \epsilon$ (open chain), with $j_0 = \lfloor N/2 \rfloor$.

4.3 Witness lower bound

We interpret $\kappa(\epsilon)$ as an effective dissipation-rate envelope for observables supported at separation ϵ within the chosen $\omega = 0$ witness sector. Let σ be a reference Gibbs/KMS state and define the KMS inner product

$$\langle A, B\rangle_\sigma \;:=\; \mathrm{Tr}(\sigma^{1/2} A^\dagger \sigma^{1/2} B), \qquad \|A\|_{2,\sigma}^2 := \langle A, A\rangle_\sigma.$$

A commutator witness yields a lower bound on an effective decay envelope:

$$\kappa(\epsilon) \;\geq\; \kappa_{\min}(\epsilon) \;:=\; \frac{\gamma(0)}{2}\, R_{\mathrm{opt}}(\epsilon), \qquad R_{\mathrm{opt}}(\epsilon) \;:=\; \max_{O\in\mathcal{A}_\epsilon} \frac{\|[S(0),O]\|_{2,\sigma}^2}{\|O\|_{2,\sigma}^2}.$$

Thus any $R_{\mathrm{opt}}(\epsilon) > 0$ implies a strictly positive certified lower bound $\kappa_{\min}(\epsilon) > 0$ whenever $\gamma(0) > 0$.

4.4 Exact diagonalization illustration and robustness

We compute $R_{\mathrm{opt}}(\epsilon)$ by exact diagonalization at $N = 10$ for $\beta \in \{0.5, 1, 2\}$ and $\gamma(0) = 0.1$. We optimize over traceless Pauli strings on a one-site block $L = 1$ (dimension $4^1 - 1 = 3$) and a two-site block $L = 2$ (dimension $4^2 - 1 = 15$). Across $\beta \in \{0.5, 1, 2\}$, the witness-based lower bound ranges

$$\kappa_{\min}(\epsilon) \sim 3.2 \times 10^{-4}\text{–}1.2 \times 10^{-3} \quad (L = 1), \qquad \kappa_{\min}(\epsilon) \sim 8.2 \times 10^{-4}\text{–}2.9 \times 10^{-3} \quad (L = 2),$$

demonstrating a robust, strictly positive $\omega = 0$ floor mechanism when $\gamma(0) > 0$.

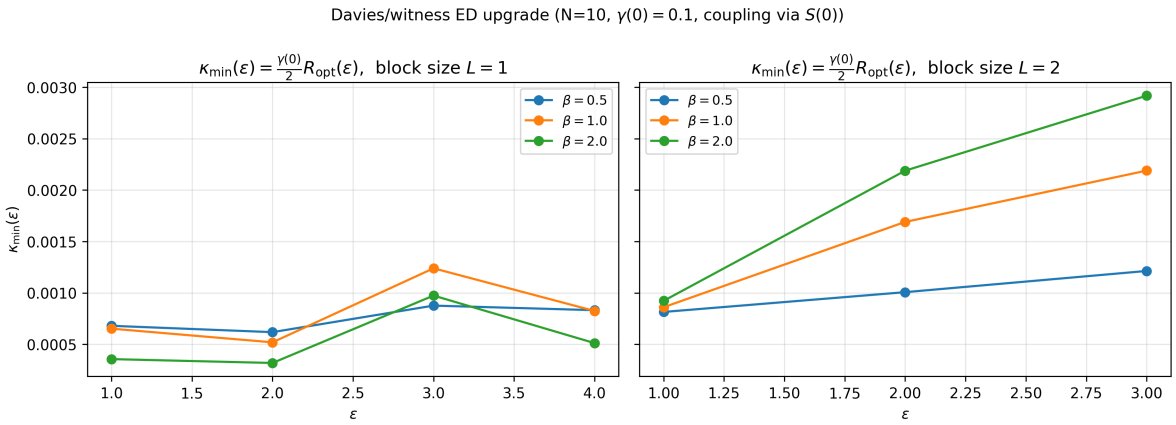

Figure 4: Davies/witness ED upgrade ($N = 10$): witness-based lower bound $\kappa_{\min}(\epsilon) = \frac{\gamma(0)}{2} R_{\mathrm{opt}}(\epsilon)$ with $\gamma(0) = 0.1$, shown for one-site ($L = 1$) and two-site ($L = 2$) observable supports and for $\beta \in \{0.5, 1, 2\}$.

5 Discussion and conclusions

The TFIM surrogate results show that, for this operational one-site trace-distance proxy in the explored regimes, an offset parameter D_0 is not supported/identifiable under either dephasing (deep tail, $N = 80$) or amplitude damping (corroborating check, $N = 24$). At the same time, the observed non-monotonicity in ϵ suggests that coherent finite-size structure can dominate the shape of $D_{\mathrm{tr}}^{\mathcal{A}}(\epsilon)$, limiting the interpretability of strictly monotone envelope fits.

In contrast, the Davies/witness stress test demonstrates an explicit and referee-proof floor mechanism (as a witness-based lower bound) when $\gamma(0) > 0$: the $\omega = 0$ component $S(0)$ is generally nonlocal in the site basis, enabling commutators with distant local observables and producing $\kappa_{\min}(\epsilon) > 0$. Together, these results highlight that floors are not universal across operational proxies, and that low-frequency bath structure and the chosen observable family determine whether a floor is detectable.

References

[1] Elliott H. Lieb and Derek W. Robinson. The finite group velocity of quantum spin systems. *Communications in Mathematical Physics*, 28:251–257, 1972.

[2] E. Brian Davies. Markovian master equations. *Communications in Mathematical Physics*, 39:91–110, 1974.

[3] Heinz-Peter Breuer and Francesco Petruccione. *The Theory of Open Quantum Systems*. Oxford University Press, 2002.

[4] Herbert Spohn. Entropy production for quantum dynamical semigroups. *Journal of Mathematical Physics*, 19:1227–1230, 1978.

[5] Kenneth P. Burnham and David R. Anderson. *Model Selection and Multimodel Inference: A Practical Information-Theoretic Approach*. Springer, 2 edition, 2002.

[6] Clifford M. Hurvich and Chih-Ling Tsai. Regression and time series model selection in small samples. *Biometrika*, 76:297–307, 1989.